Appendix A
Benchmark Model of Large Transport Aircraft

A.1 RECOVER Benchmark Model

The RECOVER (REconfigurable COntrol for Vehicle Emergency Return) benchmark model [1], which runs in the MATLAB/SIMULINK environment has been used in the Group for Aeronautical Research and Technology in Europe Flight Mechanics Action Group (GARTEUR FM-AG16). The purpose of the FM-AG16 project [1] was to conduct research in Europe to develop advanced FTC schemes for aerospace applications to cope with realistic malfunctions in actuators, sensors and control surfaces. The RECOVER model consists of 77 states and includes four engines and 25 other control surfaces (four elevators, one stabiliser, four ailerons, 12 spoilers and flaps). The RECOVER aircraft model includes realistic sensor and actuator models with realistic limits and aerodynamic effects (such as blowdown). The RECOVER software has the ability to test actuator fault/failure scenarios (elevator jam, stabiliser runaway, aileron jam and rudder runaway) and also includes the EL AL flight 1862 failure case. This software is an upgraded version of Delft University's Aircraft Simulation and Analysis Tool, DASMAT, and Flight lab 747 FTLAB747 [2]. In the upgraded version [3], the mechanically linked control surfaces (inherited from the original B747-100/200 aircraft) have been removed and replaced by individually controlled surfaces similar to more modern aircraft which use fly-by-wire systems. The removal of the mechanical link allows more flexibility in terms of fault tolerant control by creating a highly redundant system which is suitable to test state-of-the-art FTC schemes. The RECOVER software [2–4], used in this book has been used by many researchers [5–9] and is a validated benchmark platform for research in the fields of FTC and FDI.

The rigid body states of the B747-100/200 aircraft for the longitudinal, lateral and directional axis are

$$x(t) = (p, q, r, V_{tas}, \alpha, \beta, \phi, \theta, \psi, h_e, x_e, y_e) \tag{A.1}$$

M.T. Hamayun et al., *Fault Tolerant Control Schemes Using Integral Sliding Modes*, Studies in Systems, Decision and Control 61,
DOI 10.1007/978-3-319-32238-4

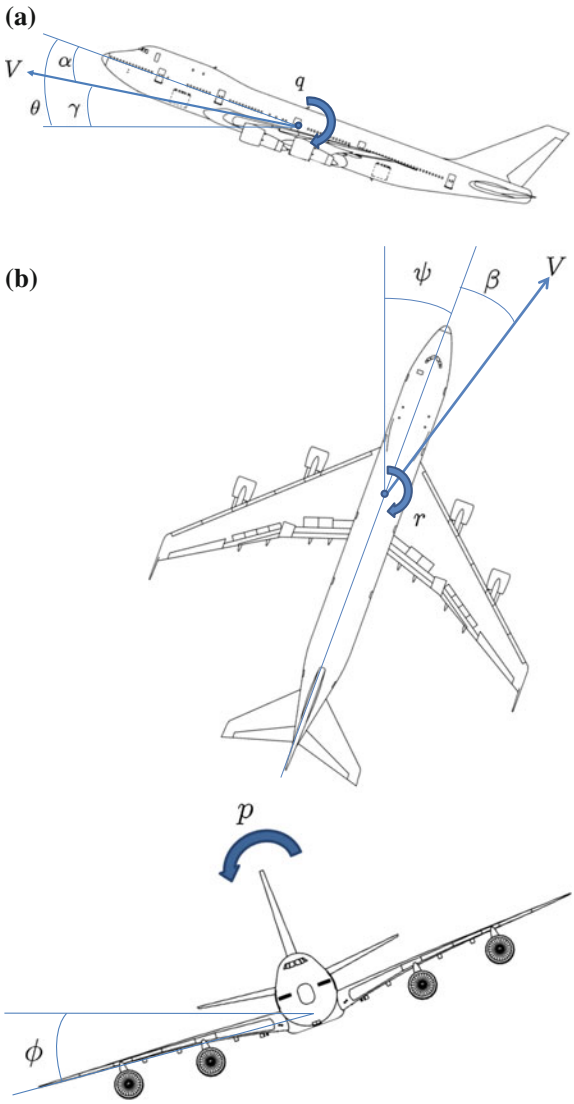

Fig. A.1 Aircraft attitudes (adapted from [1]). **a** Longitudinal. **b** Lateral and directional

which are determined from the 6-DOF equations. In Eq. A.1 the states for the longitudinal axis (Fig. A.1a) are $x_{long} = (q, V_{tas}, \alpha, \theta, h_e)$, which represent pitch rate q (rad/s), true air speed V_{tas} (m/s), angle of attack α (rad), pitch angle θ (rad) and altitude h_e (m). On the other hand the states for the lateral and directional axis (Fig. A.1b) are $x_{lat} = (p, r, \beta, \phi, \psi)$, which represent roll rate p (rad/s), yaw rate r (rad/s), sideslip β (rad), roll angle ϕ (rad) and yaw angle ψ (rad). In Eq. (A.1), the states (h_e, x_e, y_e) represent geometric earth position, along the z-axis, x-axis and y-axis respectively. The typical control surfaces for the longitudinal and lateral axis control

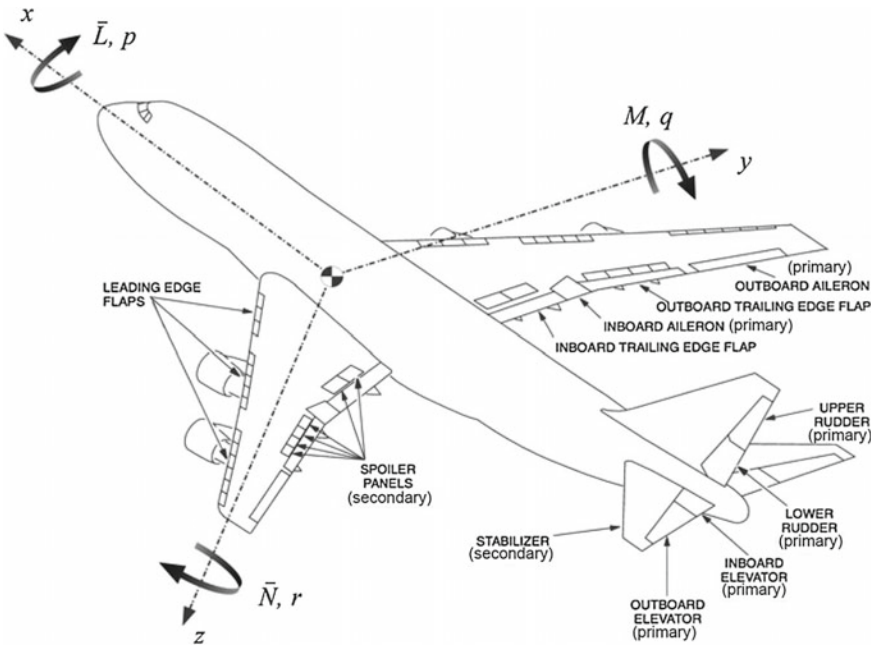

Fig. A.2 Boeing 747 flight control surface arrangements and body axes and moment definitions (L = rolling moment, M = pitching moment, N = yawing moment, p = roll rate, q = pitch rate, r = yaw rate) (Figure adapted from [1])

are shown in Fig. A.2. The control surfaces which are typically used for longitudinal axis control comprise 4 elevators (inboard and outboard), a horizontal stabiliser, 4 engines thrusts (two on each wing), which can be controlled through the Engine Pressure Ratio (EPR). For lateral axis control, 4 ailerons (inboard and outboard on each wing), 12 spoilers (2 inboard and 4 outboard spoilers on each wing), 2 rudders (upper and lower), and 4 engines thrusts (controlled through EPR) are used. A linear state-space model of the RECOVER benchmark can be obtained at a given trim point. At the trim point, the aircraft is in steady state for example straight and level flight. In this book the longitudinal and lateral axis of the benchmark model, at different trim conditions, is considered as the basis for designing the FTC schemes. For example in Chaps. 3 and 5, the simulations are based around an operating condition of straight and level flight at 263,000 kg, 92.6 m/s true airspeed, and at an altitude of 600 m based on 25.6 % of maximum thrust and at a 20 deg flap position. The result is a 12th order linear model, which can be divided into two six order models for longitudinal and lateral axis control. The first four states $x_{long} = (q, V_{tas}, \alpha, \theta)$ and $x_{lat} = (p, r, \beta, \phi)$ are used for the controller design. At this trim condition the state-space matrices are:

$$A_{long} = \begin{bmatrix} -0.5137 & 0.0004 & -0.5831 & 0 \\ 0 & -0.0166 & 1.7171 & -9.8046 \\ 1.0064 & -0.0021 & -0.6284 & 0 \\ 1.0000 & 0 & 0 & 0 \end{bmatrix} \tag{A.2}$$

$$B_{long} = \begin{bmatrix} -0.6228 & -1.3578 & 0.0082 & 0.0218 & 0.0218 & 0.0082 \\ 0 & -0.1756 & 1.4268 & 1.4268 & 1.4268 & 1.4268 \\ 0.0352 & -0.0819 & 0.0021 & -0.0021 & -0.0021 & -0.0021 \\ 0 & 0 & 0 & 0 & 0 & 0 \end{bmatrix} \tag{A.3}$$

$$A_{lat} = \begin{bmatrix} -1.0579 & 0.1718 & -1.6478 & 0.0004 \\ 0.1186 & -0.2066 & 0.2767 & -0.0019 \\ 0.1014 & -0.9887 & -0.0999 & 0.1055 \\ 1.0000 & 0.0893 & 0 & 0 \end{bmatrix} \tag{A.4}$$

$$B_{lat} = \begin{bmatrix} -0.0832 & 0.0832 & -0.2285 & 0.2285 & -0.2625 & -0.0678 & 0.0678 \\ -0.0154 & 0.0154 & -0.0123 & 0.0123 & -0.0180 & -0.0052 & 0.0052 \\ 0 & 0 & 0 & 0 & 0.0017 & 0.0006 & -0.0006 \\ 0 & 0 & 0 & 0 & 0 & 0 & 0 \\ 0.2625 & 0.1187 & 0.0246 & 0.0140 & -0.0140 & -0.0246 & \\ 0.0180 & -0.2478 & 0.1269 & 0.0724 & -0.0724 & -0.1269 & \\ -0.0017 & 0.0174 & 0.0005 & 0.0005 & -0.0005 & -0.0005 & \\ 0 & 0 & 0 & 0 & 0 & 0 & \end{bmatrix} \tag{A.5}$$

where the control surfaces for the longitudinal axis are

$$\delta_{long} = (\delta_e, \delta_s, e1_{long}, e2_{long}, e3_{long}, e4_{long}) \tag{A.6}$$

which represent elevator deflection (rad) (4 elevators are aggregated to produce one control input), horizontal stabiliser deflection (rad) and four longitudinal engines pressure ratios. For lateral axis control the control surfaces comprise

$$\delta_{lat} = (\delta_{air}, \delta_{ail}, \delta_{aor}, \delta_{aol}, sp_{1-4}, sp_5, sp_8, sp_{9-12}, \delta_r, e1_{lat}, e2_{lat}, e3_{lat}, e4_{lat}) \tag{A.7}$$

which represent aileron inboard (right and left) deflection (rad), aileron outboard (right and left) deflection (rad), left wing spoiler deflections (rad) ($sp_1 - sp_4$, sp_5), right wing spoiler deflections (rad) (sp_8, $sp_9 - sp_{12}$), rudder deflection (rad) (the upper and lower rudders are aggregated to produce one control input) and four lateral engine pressure ratios. The spoilers sp_6 and sp_7 are ground spoilers and are not used in flight. Further details of the RECOVER model can be found in [1, 2] and the references therein.

A.1.1 LPV Plant of a RECOVER Benchmark Model

The LPV plant representation of the RECOVER model used for longitudinal controller design is obtained from [10], where the LPV model is approximated by polynomially fitting the aerodynamic coefficients obtained from [11] to create an LPV representation using the function substitution method. The aerodynamic coefficients are polynomial functions of velocity V_{tas} and angle of attack α in the range of $\left[\,150,\ 250\,\right]$ m/s and $\left[\,-2,\ 8\,\right]$ deg respectively and at the altitude of 7000 m. The states of the LPV plant are $(\bar{\alpha}, \bar{q}, \bar{V}_{tas}, \bar{\theta}, \bar{h}_e)$ which represent *deviation* of the angle of attack, pitch rate, true air speed, pitch angle and altitude from their trim values. The inputs of the LPV plant are $(\bar{\delta_e}, \bar{\delta_s}, \bar{T_n})$, which represent deviation of elevator deflection, horizontal stabiliser deflection and total engine thrust from their trim values respectively. The trim values of the states are

$$(\alpha_{trim}, q_{trim}, V_{tas_{trim}}, \theta_{trim}, h_{e_{trim}}) = (1.05\,\text{deg}, 0\,\text{deg/s}, 227.02\,\text{m/s}, 1.05\,\text{deg}, 7000\,\text{m})$$

and the trim values of the LPV plant inputs are

$$(\delta_{e_{trim}}, \delta_{s_{trim}}, T_{n_{trim}}) = (0.163\,\text{deg}, 0.590\,\text{deg}, 42291\,\text{N})$$

The LPV system matrices are given by

$$A(\rho) = A_0 + \sum_{i=1}^{7} \rho_i A_i \quad \text{and} \quad B(\rho) = B_0 + \sum_{i=1}^{7} \rho_i B_i \tag{A.8}$$

where

$$(\rho_1, \ldots, \rho_7) := (\bar{\alpha}, \bar{V}_{tas}, \bar{V}_{tas}\bar{\alpha}, \bar{V}_{tas}^2, \bar{V}_{tas}^2\bar{\alpha}, \bar{V}_{tas}^3, \bar{V}_{tas}^4)$$

where $\bar{\alpha} = \alpha - \alpha_{trim}$ and $\bar{V}_{tas} = V_{tas} - V_{tas_{trim}}$. After reordering, the LPV plant states for the control law design become $(\bar{\theta}, \bar{\alpha}, \bar{V}_{tas}, \bar{q})$. The LPV system matrix is given by

$$A(\rho) = \begin{bmatrix} 0 & 0 & 0 & a_{14}(\rho) \\ 0 & a_{33}(\rho) & a_{32}(\rho) & a_{34}(\rho) \\ a_{21}(\rho) & a_{23}(\rho) & a_{22}(\rho) & 0 \\ 0 & a_{43}(\rho) & a_{42}(\rho) & a_{44}(\rho) \end{bmatrix} \tag{A.9}$$

where

$$\begin{aligned} a_{14}(\rho) &= 1 \\ a_{33}(\rho) &= -0.5935 - 2.5923 \times 10^{-3}\rho_2 \\ a_{32}(\rho) &= -5.2124 \times 10^{-4} - 6.2678 \times 10^{-7}\rho_2 + 1.1121 \times 10^{-11}\rho_4 \\ a_{34}(\rho) &= 0.9914 \end{aligned}$$

$$
\begin{aligned}
a_{21}(\rho) &= -9.7851 \\
a_{23}(\rho) &= 5.7733 - 84.5625\rho_1 - 3.5127 \times 10^{-2}\rho_2 - 0.7450\rho_3 - 0.7736 \times 10^{-4}\rho_4 \\
&\quad -1.6408 \times 10^{-3}\rho_5 \\
a_{22}(\rho) &= -6.1168 \times 10^{-3} - 2.1091 \times 10^{-5}\rho_2 - 2.2374 \times 10^{-8}\rho_4 \\
a_{43}(\rho) &= -1.9626 + 3.4170\rho_1 - 0.01729\rho_2 + 0.0301\rho_3 - 0.38081 \times 10^{-4}\rho_4 \\
&\quad +6.630 \times 10^{-5}\rho_5 \\
a_{42}(\rho) &= -4.9579 \times 10^{-4} - 3.8893 \times 10^{-6}\rho_2 - 7.6201 \times 10^{-9}\rho_4 \\
&\quad +0.19644 \times 10^{-11}\rho_6 \\
a_{44}(\rho) &= -0.46087 - 0.00203\rho_2
\end{aligned}
$$

and the LPV input distribution matrix is

$$
B(\rho) = \begin{bmatrix} 0 & 0 & 0 \\ b_{31}(\rho) & b_{32}(\rho) & b_{33}(\rho) \\ 0 & 0 & b_{23}(\rho) \\ b_{41}(\rho) & b_{42}(\rho) & b_{43}(\rho) \end{bmatrix} \tag{A.10}
$$

where

$$
\begin{aligned}
b_{31}(\rho) &= -0.0358 - 1.1877 \times 10^{-5}\rho_2 + 1.5311 \times 10^{-6}\rho_4 + 3.9135 \times 10^{-9}\rho_6 \\
b_{32}(\rho) &= -0.0716 \\
b_{33}(\rho) &= -3.6326 \times 10^{-4} - 5.8732 \times 10^{-3}\rho_1 + 1.6002 \times 10^{-6}\rho_2 \\
&\quad +0.25871 \times 10^{-4}\rho_3 \\
b_{23}(\rho) &= 1.3323 - 0.058133\rho_1 \\
b_{41}(\rho) &= -1.7696 - 0.0089\rho_2 + 0.5985 \times 10^{-4}\rho_4 + 0.4428 \times 10^{-6}\rho_6 \\
&\quad +0.6912 \times 10^{-9}\rho_7 \\
b_{42}(\rho) &= -3.9993 - 0.035233\rho_2 - 0.776 \times 10^{-4}\rho_4 \\
b_{43}(\rho) &= 0.015328.
\end{aligned}
$$

References

1. Edwards, C., Lombaerts, T., Smaili, H.: Fault Tolerant Flight Control: A Benchmark Challenge. Springer, Berlin (2010)
2. Marcos, A., Balas, G.J.: A Boeing 747-100/200 aircraft fault tolerant and diagnostic benchmark. Technical Report AEM–UoM–2003–1, Department of Aerospace and Engineering Mechanics, University of Minnesota (2003)
3. Smaili, M., Breeman, J., Lombaerts, T., Joosten, D.: A simulation benchmark for integrated fault tolerant flight control evaluation. In: AIAA Modeling and Simulation Technologies Conference and Exhibit (2006)
4. van der Linden C.M.: DASMAT Delft University Aircraft Simulation Model and Analysis Tool. Technical Report LR-781, Delft University of Technology, Delft, The Netherlands (1996)

5. Alwi, H., Edwards, C., Tan, C.P.: Fault Detection and Fault Tolerant Control Using Sliding Modes. Advances in Industrial Control Series. Springer, Berlin (2011)
6. Wang, T., Xiey, W., Zhang, Y.: Adaptive sliding mode fault tolerant control of civil aircraft with separated uncertainties. In: 48th AIAA Aerospace Sciences Meeting Including the New Horizons Forum and Aerospace Exposition, pp. 1–9 (2010)
7. Ganguli, S., Marcos, A., Balas, G.J.: Reconfigurable LPV control design for Boeing 747-100/200 longitudinal axis. In: Proceedings of the American Control Conference (2002)
8. Alwi, H., Edwards, C.: Robust actuator fault reconstruction for LPV systems using sliding mode observers. In: Proceedings of the 49th IEEE Conference on Decision and Control, pp. 84–89 (2010)
9. Henning, A., Balas, G.J.: MPC supervisory flight controller: a case study to flight EL AL 1862. In: AIAA Guidance, Navigation and Control Conference and Exhibit, pp. 1–17 (2008)
10. Khong, T.H., Shin, J.: Robustness analysis of integrated LPV-FDI filters and LTI-FTC system for a transport aircraft. In: AIAA Guidance, Navigation, and Control Conference and Exhibit, AIAA-2007-6771 (2007)
11. Marcos, A., Balas, G.J.: Development of linear-parameter-varying models for aircraft. AIAA J. Guid. Control Dyn. **27**(2), 218–228 (2004)

Appendix B
Closed-Loop Stability and Feedback Gain Synthesis

B.1 $\mathscr{L}_2$ Gain and Small Gain Theorem

B.1.1 $\mathscr{L}_2$ Gain

In the case of LTI systems the $\mathscr{L}_2$ gain can be calculated accurately [1]. Consider a LTI system

$$\dot{x}(t) = Ax(t) + Bu(t)$$
$$y(t) = Cx(t) + Du(t)$$

where it is assumed that the system matrix A is *Hurwitz*. The system above can be written as $G(s) = C(sI - A)^{-1}B + D$, then according to Theorem 6.4 in [2], the $\mathscr{L}_2$ gain of the system $G(s)$ is $\sup_{\omega \in \mathbf{R}} \|G(\, j\omega)\|_2$, which is the induced 2-norm of the system $G(j\omega)$. The $\mathscr{L}_2$ gain of the system in the time domain is equal to the $\mathscr{H}_\infty$ norm in the frequency domain [2], which means if $Y(j\omega) = G(j\omega)U(j\omega)$, then from Theorem 6.4 [2] it is shown that

$$\|y\|_{\mathscr{L}_2}^2 \leq (\sup_{\omega \in \mathbf{R}} \|G(j\omega)\|_2)^2 \|u\|_{\mathscr{L}_2}^2 \tag{B.1}$$

where $\|u\|_{\mathscr{L}_2}^2 = \int_0^\infty u^T(t)u(t)dt$.

B.1.2 Small Gain Theorem

The small gain theorem is a systematic approach to investigate the input-output stability of interconnected dynamical systems [2]. Consider the feedback interconnection in Fig. B.1. Suppose that e_1 is the input to system H_1 and y_1 is the output,

M.T. Hamayun et al., *Fault Tolerant Control Schemes Using Integral Sliding Modes*, Studies in Systems, Decision and Control 61,
DOI 10.1007/978-3-319-32238-4

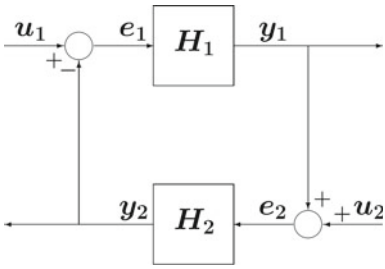

Fig. B.1 Feedback interconnection of two systems (adapted from [2])

then the system H_1 is finite gain $\mathscr{L}_2$ stable if $\|y_1\|_{\mathscr{L}_2} \leq \gamma_1 \|e_1\|_{\mathscr{L}_2}$. Now consider the interconnection of two systems as shown in Fig. B.1, then according to the small gain theorem [2], with the assumption that the two systems H_1 and H_2 are finite gain $\mathscr{L}_2$ stable, with $\mathscr{L}_2$ gains γ_1 and γ_2 respectively, then the feedback connection will be finite gain $\mathscr{L}_2$ stable if

$$\gamma_2 \gamma_1 < 1 \tag{B.2}$$

The proof can be found in [2].

B.2 LMI Equivalence of Closed-Loop Stability Analysis

To satisfy the stability condition of Theorem 3.1 in Chap. 3, a closed-loop analysis is carried out in an LMI framework, in order to find a feedback gain F such that the $\mathscr{H}_\infty$ norm of the transfer function $\tilde{G}(s) = F(sI - \tilde{A})^{-1}\tilde{B}$ is less than some predefined scalar γ i.e. $\|\tilde{G}(s)\|_\infty < \gamma$. Two constraints are imposed on the design of the feedback gain F which need to be satisfied simultaneously. Firstly to achieve (nominal) performance, an LQR formulation is used; and secondly, to ensure the design of an F to satisfy the stability condition of Theorem 3.1, a Bounded Real Lemma (BRL) formulation is used.

B.2.1 LMI Formulation of the LQR problem

In Sect. 3.2.4 the design of the feedback gain F is based on the nominal system in (3.18). For the LMI formulation of the LQR problem, consider the LTI system

$$\dot{x}(t) = Ax(t) + B_v v(t) \tag{B.3}$$

$$z(t) = Q_1 x(t) + R_1 v(t) \tag{B.4}$$

where v represents the (virtual) control input and Q_1 and R_1 are symmetric positive definite matrices where $Q_1^T R_1 = 0$. The LQR problem involves determining the

control law $v(t) = -Fx(t)$ such that $J = \int_0^\infty z^T z$ is minimised. Consider the Lyapunov function $V(x) = x^T Px$ where $P > 0$ and assume the inequality

$$\dot{V} + z^T z \leq 0 \qquad \text{holds for all } x \text{ and } z \tag{B.5}$$

Integrating (B.5) yield the expression

$$J = \int_0^\infty z^T z \leq V(0) - V(\infty)$$

Since a stabilising gain F is required, $x(t) \to 0$ as $t \to \infty$ and $V(\infty) = 0$. Therefore

$$J \leq x^T(0)Px(0)$$

Clearly the cost J depends on the specific initial condition $x(0)$. If $x(0)$ is treated as a random variable with zero mean, then[1]

$$\begin{aligned} \mathbb{E}(J) &\leq \mathbb{E}\left(\text{trace}\left(x^T(0)Px(0)\right)\right) \\ &= \text{trace}\left(\mathbb{E}\left(x^T(0)Px(0)\right)\right) \\ &= \text{trace}(P)\text{Var}\left(x(0)\right) \end{aligned} \tag{B.6}$$

where $\text{Var}(\cdot)$ represents the variance of a random variable. From (B.6) minimising $\text{trace}(P)$ subject to (B.5) is an appropriate approach.

Taking the time derivative of $V(x)$ and substituting from (B.3) yields

$$\dot{V} = x^T(PA + A^T P)x + x^T PB_v v + v^T B_v^T Px$$

Substituting the value of $\dot{V}$ above and (B.4) into (B.5), implies the inequality in (B.5) is equivalent to

$$PA + A^T P + Q_1^T Q_1 - PB_v F - F^T B_v^T P - Q_1^T R_1 F - F^T R_1^T Q_1 + F^T R_1^T R_1 F < 0 \tag{B.7}$$

Inequality (B.7), is clearly not convex [1], and cannot be written as an LMI representation. Define $X = P^{-1}$ then by pre and post multiplying the inequality in (B.7) by X together with the change of variable $Y = FX$, implies inequality (B.7) can be written as

$$AX + XA^T + X^T Q_1^T Q_1 X - B_v Y - Y^T B_v^T - X^T Q_1^T R_1 Y - Y^T R_1^T Q_1 X + Y^T R_1^T R_1 Y < 0 \tag{B.8}$$

[1] Here $\mathbb{E}(\cdot)$ is the mathematical expectation operator, and in establishing (B.6) the fact that the linear operators $\mathbb{E}(\cdot)$ and $\text{trace}(\cdot)$ commute is exploited [3].

Finally using the Schur complement [1], inequality (B.8) can be written as

$$\begin{bmatrix} AX + XA^T - B_v Y - Y^T B_v^T & (Q_1 X - R_1 Y)^T \\ (Q_1 X - R_1 Y) & -I \end{bmatrix} < 0 \tag{B.9}$$

where the matrices X and Y are the decision variables. The requirement now is to minimise trace(X^{-1}). From the definition of $X = P^{-1}$, using the Schur complement [1], the inequality

$$\begin{bmatrix} -Z & I \\ I & -X \end{bmatrix} < 0 \tag{B.10}$$

implies $X^{-1} < Z$ and therefore

$$\text{trace}(Z) > \text{trace}(X^{-1}) \tag{B.11}$$

The overall problem then becomes:

Minimise trace(Z) subject to (B.10) and (B.9).

Once X and Y are synthesised, the feedback gain F can be recovered as $F = YX^{-1}$.

B.2.2 LMI Formulation of the BRL

In Sect. 3.2.2, the closed-loop stability of the sliding motion is governed by

$$\dot{x}(t) = \underbrace{(A - B_v F)}_{\tilde{A}} x(t) + \tilde{B}\vartheta(t) \tag{B.12}$$

$$z(t) = Fx(t) \tag{B.13}$$

where $\vartheta(t) = \Phi(t)z(t)$. The $\mathscr{L}_2$ gain from ϑ to z (which in this LTI situation is the $\mathscr{H}_\infty$ norm of $\tilde{G}(s) = F\left(sI - \tilde{A}\right)^{-1}\tilde{B}$) is less than γ if there exists a Lyapunov function $V(x) = x^T P x$ where $P > 0$ such that

$$\int_0^\infty (\dot{V}(\tau) + z^T z - \gamma^2 \vartheta^T \vartheta) d\tau < 0 \qquad \text{for all } x \text{ and } \vartheta \tag{B.14}$$

holds, since rearranging the inequality in (B.14) and assuming $x(0) = 0$ yields

$$\int_0^\infty z^T z < \gamma^2 \int_0^\infty \vartheta^T \vartheta - V(\infty) \leq \gamma^2 \int_0^\infty \vartheta^T \vartheta$$

To guarantee (B.14) holds, the inequality

$$\dot{V} + z^T z - \gamma^2 \vartheta^T \vartheta < 0 \tag{B.15}$$

for all x and ϑ will be enforced.[2] Taking the time derivative of the function $V(x)$ and substituting from (B.12) yields

$$\dot{V} = x^T (P(A - B_v F) + (A - B_v F)^T P)x + \vartheta^T \tilde{B}^T P x + x^T P \tilde{B} \vartheta$$

Substituting $\dot{V}$ and (B.13) into (B.15) means (B.15) is equivalent to

$$x^T (P(A - B_v F) + (A - B_v F)^T P)x + \vartheta^T \tilde{B}^T P x + x^T P \tilde{B} \vartheta + x^T F^T F x - \gamma^2 \vartheta^T \vartheta < 0$$

which can be written as

$$\begin{bmatrix} x \\ \vartheta \end{bmatrix}^T \begin{bmatrix} P(A - B_v F) + (A - B_v F)^T P + F^T F & P\tilde{B} \\ \tilde{B}^T P & -\gamma^2 I \end{bmatrix} \begin{bmatrix} x \\ \vartheta \end{bmatrix} < 0 \tag{B.16}$$

or in other words

$$\begin{bmatrix} P(A - B_v F) + (A - B_v F)^T P + F^T F & P\tilde{B} \\ \tilde{B}^T P & -\gamma^2 I \end{bmatrix} < 0 \tag{B.17}$$

Inequality (B.17) can be written as

$$\begin{bmatrix} P(A - B_v F) + (A - B_v F)^T P & P\tilde{B} \\ \tilde{B}^T P & -\gamma^2 I \end{bmatrix} + \begin{bmatrix} F^T \\ 0 \end{bmatrix} \begin{bmatrix} F & 0 \end{bmatrix} < 0 \tag{B.18}$$

which from the Schur complement [1], is equivalent to

$$\begin{bmatrix} P(A - B_v F) + (A - B_v F)^T P & P\tilde{B} & F^T \\ \tilde{B}^T P & -\gamma^2 I & 0 \\ F & 0 & -I \end{bmatrix} < 0 \tag{B.19}$$

[2] See page 122 of [1].

From Eq. (B.19) it is clear that the expression in the top left position is not convex and cannot be written as an LMI representation. However multiplying both sides of (B.19) by $\text{diag}(P^{-1}, I, I)$ means (B.19) is equivalent to

$$\begin{bmatrix} (A - B_v F)P^{-1} + P^{-1}(A - B_v F)^T P & \tilde{B} & P^{-1}F^T \\ \tilde{B}^T & -\gamma^2 I & 0 \\ FP^{-1} & 0 & -I \end{bmatrix} < 0 \tag{B.20}$$

Letting $P^{-1} = X$, the inequality in (B.20) is equivalent to

$$\begin{bmatrix} (A - B_v F)X + X(A - B_v F)^T P & \tilde{B} & XF^T \\ \tilde{B}^T & -\gamma^2 I & 0 \\ FX & 0 & -I \end{bmatrix} < 0 \tag{B.21}$$

Finally with the change of variable $Y = FX$, inequality (B.21) can be written as

$$\begin{bmatrix} AX + XA - B_v Y - Y^T B_v^T & \tilde{B} & Y^T \\ \tilde{B}^T & -\gamma^2 I & 0 \\ Y & 0 & -I \end{bmatrix} < 0 \tag{B.22}$$

where the matrices X and Y represent the decision variables. Inequality (B.22) is convex and available LMI tools can be used to find a feasible solution. The gain matrix F can be recovered using the relation $F = YX^{-1}$.

References

1. Boyd, S.P., Ghaoui, L., Feron, E., Balakrishnan, V.: Linear Matrix Inequalities in System and Control Theory. Society for Industrial and Applied Mathematics, Philadelphia (1994)
2. Khalil, H.K.: Nonlinear Systems. Prentice Hall, Upper Saddle River (1992)
3. Byrne, C.L.: Signal Processing: A Mathematical Approach, 2nd Edition. CRC Press, Boca Raton (2014)

Index

Symbols
$\mathscr{H}_\infty$ control, 8, 10, 11, 79, 101, 120, 166
$\mathscr{H}_\infty$ norm, 47, 50, 68, 88, 189, 190, 192
$\mathscr{L}_2$ gain, 47, 50, 110, 155, 189, 192
μ-synthesis, 79

A
A posteri approach, ix, 103, 113, 120
A priori, 105, 112, 114, 115
Active fault tolerant control, viii, xiv, 6, 7, 9, 11, 12, 167
Actuator channel, ix, 49
Actuator effectiveness gain, 39, 129
Actuator effectiveness matrix, xiii, 70, 82, 154
Actuator efficiency, 12, 40, 45, 133, 136, 156
Actuator failures, viii, 12, 34, 49, 59, 135, 163
Actuator faults, viii, 1, 8, 34, 36, 49, 60, 101, 146, 153, 167
Actuator redundancy, 11, 35, 41, 150
Adaptation scheme, 158
Adaptive, 79, 101, 120, 149, 158, 171, 178
Adaptive control, 10
Adaptive gain, 156, 158, 163, 166, 173, 175, 178
Adaptive modulation function, 156
Affine, 89, 150, 152, 159
Aileron jam, 181
Allocation matrix, 130, 132, 146
Analytical redundancy, 6
Augmentation scheme, ix, 103, 107
Availability, vii, 39, 59, 73, 99

B
Backstepping, ix, 123, 125, 128, 134, 136, 143, 146
Baseline controller, ix, 27, 106, 109, 113, 116, 120, 123, 128, 132
Bias fault, 3
Bounded real lemma, 50, 70, 88, 160, 190
Boundedness of pseudo-inverses, 43

C
Chattering, 25, 30, 33, 36
Civil aircraft benchmark model, 81, 92
Closed-loop sliding motion, 27, 109, 110, 154, 155
Component fault, ix, viii, 1, 2, 81
Component level, viii, 3, 81
Condition number, 154
Control action, 4, 9, 41, 52, 82, 151
Control allocation, viii, ix, xiv, 10–12, 35, 36, 39, 42, 43, 59, 60, 63–65, 73, 78, 79, 81, 82, 100, 103, 106, 111, 117, 120, 123, 129–131, 143, 146, 149, 166, 178
Control effectiveness level estimation, 6
Control loop, ix, 35, 103, 126, 134
Control surface, 39, 51, 59, 73, 93, 113–115, 123–128, 131, 133, 134, 136, 140, 146, 159, 166, 169, 171, 173, 179, 181–184
Controllability, 105, 152
Controllable, 7, 18, 40, 41, 50, 52, 65, 83, 89, 104, 105, 127, 151, 152
Controlled outputs, 40, 51, 64, 161
Controller gain, 50, 53, 88, 100
Cost function, 33, 50, 159

M.T. Hamayun et al., *Fault Tolerant Control Schemes Using Integral Sliding Modes*, Studies in Systems, Decision and Control 61,
DOI 10.1007/978-3-319-32238-4

D
Daisy chaining, 12, 60
Decision variable, 50, 89, 160, 192, 194
Decoupled, 116, 143, 162
Direct CA, 73
Directional axis, 181
Discontinuous, 20, 25, 27, 31, 55, 56, 156
Disturbance, vii, 6, 8, 17, 18, 20, 22, 24, 27, 29, 30, 32, 63, 120, 126, 127
Dominant contribution, 41, 52, 151
Drift fault, 3
DUECA, 170
Dutch roll mode, 115
Dynamic inversion, 10

E
Effectiveness, viii, 5, 6, 39, 40, 46, 47, 49, 54, 59, 63, 64, 78, 81, 82, 100, 103, 104, 106, 115, 116, 120, 127, 129, 132, 140, 149, 159, 163, 166, 175, 178
Efficiency, 6, 40, 43, 150
Eigenstructure, 11, 114
Eigenstructure assignment, 101, 113–115, 120
EL AL flight 1862, 181
Elevator float, 136, 140, 143
Elevator jam, 73, 99, 140, 143, 163, 172, 175, 181
Engine pressure ratio (EPR), xiv, 51, 71, 72, 93, 126, 183, 184
Equations of motion, ix, 108, 123, 125, 130, 132, 146, 147
Equivalent control, 18–20, 29, 35, 45, 66, 67, 85, 108, 131, 153
Equivalent injection term, 56
Euclidean norm, xiii
Exogenous, 94, 127

F
False alarms, 6
Fault and failure, viii, 1, 3–5
Fault compensation, 167
Fault detection and isolation (FDI), viii, xiv, 6, 11, 12, 117, 181
Fault estimation, 6, 45, 49, 136, 167
Fault reconstruction, 11, 36, 54, 60
Fault Tolerant Control (FTC), vii, viii, xiv, 1, 3, 5–7, 11, 12, 36, 57, 59, 63–65, 71, 72, 99–101, 103, 106, 120, 123, 146, 149, 154, 163, 166, 169, 178, 179, 181, 183
Fault tolerant scheme, viii, ix, 59, 123, 146
Faults/failures, viii, ix, 4, 6, 7, 9, 11, 27, 39, 42, 46, 60, 63, 72, 78, 79, 107, 123, 126, 127, 146, 154, 163, 178
FDI information, 78, 79
FDI scheme, viii, ix, 6, 9, 11, 12, 40, 78, 81, 82, 104, 117, 120, 129, 134, 136, 159, 163, 175
Feedback gain, 28, 45, 46, 49, 51, 52, 66, 70–72, 95, 114, 155, 159, 162, 189, 190, 192
Feedback loop, 47, 68, 88, 125, 134
Finite time, 20
Flight simulator, 169
Float (failure), 3, 136, 140, 143
Fly-by-wire, 6, 178
Frozen (failure), 3
Full state information, viii, 18

G
GARTEUR FM-AG16, xiv, 79, 135, 163, 171, 173, 181
Gust, 63, 73, 78

H
Hardover (failure), 3, 99
Hardware redundancy, 10
Hedging, 36
High frequency switching, 25
Higher order sliding mode, 25, 36
Human motion perception, 178

I
Ideal sliding motion, 19–21, 24, 31, 57
Idempotent, 30
Incipient faults, 3
Input distribution matrix, ix, 5, 7, 10, 18, 27, 30, 41, 64, 81, 93, 104, 114, 149, 161, 186
Integral action, 52
Integral action states, 52, 53, 64, 161, 162
Integral sliding mode (ISM), vii, viii, ix, xiv, 11, 17, 27, 29, 31, 32, 36, 42, 43, 59, 64, 70, 83, 103, 106, 107, 111, 113, 120, 123, 131, 146, 152, 155, 166, 169, 178
Integrated, 101
Intermittent faults, 3
Invariant subspaces, 152
Invariant zeros, 101
ISMC, xiv, 27

J
Jam (failure), 3, 117, 140, 143, 175

K
Kalman filter, 6, 12, 101

L
Large transport aircraft, ix, viii, x, 39, 59, 71, 113, 134
Lateral axis, 51, 181–183
Lateral axis control, 171, 183, 184
Lateral dynamics, 113
Least squares method, 134, 171
Linear component, 93, 166, 178
Linear parameter varying (LPV), ix, xiv, 10, 149, 150, 166, 169
Linear time invariant (LTI), xiv, 4, 18
LMI, viii, ix, xiv, 39, 51, 53, 63, 72, 81, 95, 160, 162, 166, 190
LMI equivalence, 190
LMI formulation, 50, 160, 190, 192
LMI optimisation, 39, 50, 70, 89
LMI representation, 191, 194
LMI synthesis, ix, 88
LMI tool, 194
Lock in place (failure), 3, 57, 59, 140, 143
Longitudinal, 173, 184
Longitudinal axis, 135, 171, 181–183
Longitudinal control, 36, 71, 123, 171, 175, 185
Longitudinal dynamics, 72, 125
Longitudinal model, 167
Longitudinal motion, ix, 123
Longitudinal states, 173
Lookup table, 124, 126
Loss of effectiveness, 1, 5, 12, 34, 60, 120, 136
LPV controller, 166
LPV design, 171
LPV method, 149, 166
LPV model, x, 149, 160, 162, 163, 173, 185
LPV plant, ix, x, 152, 155, 160, 161, 167, 185
LPV plant states, 185
LPV representation, 167, 185
LPV system, 149, 152, 159, 166, 167, 185
LQR, xiv, 33, 120, 159, 160, 190
LQR formulation, 50, 70, 89, 190
LTI system, 28, 39, 60, 104, 149, 189, 190
Lyapunov, 32
Lyapunov function, 48, 69, 92, 112, 133, 157, 166, 191, 192
Lyapunov matrix, 50, 51, 160

M
Matched uncertainty, 18, 30, 44, 126, 132, 134
Minimum phase, 83, 89, 95
Model based, 6, 11, 12
Model free, 6
Model predictive control (MPC), xiv, 10, 79
Modulation gain, 30–32, 48, 69, 90, 91, 98, 112, 132–134, 149
Moore-Penrose pseudo-inverse, 30
Motion flight simulator, x
Moving window, 175
MRAC, xiv, 79
msfsyn, 162
Multivariable, 21

N
Nonlinear dynamic inversion, 123, 125, 178
Nonsingular, 18, 19, 29, 30, 67, 105
Null space, 64

O
Observer gain, ix, 81, 88–90, 95
Online CA, 73, 78
Online control redesign, 9
Operating condition, ix, 2, 51, 71, 93, 123, 146, 149, 173, 183
Optimal control, 12
Optimisation, 39, 51, 71, 89, 160, 162
Orthogonal, 105, 107
Output distribution matrix, 64, 82, 161
Output feedback, viii, 101, 166
Over-actuated system, 7, 63

P
Parameter uncertainty, 100
Parameter vector, 149, 150, 159
Parametric uncertainty, 81, 87
Passive approaches, 146
Passive fault tolerant control, viii, xiv, 7, 11, 12, 65, 78
Physical control law, 42, 49, 65, 70, 82, 92, 106, 113, 115, 151, 158, 159
PID, 134, 136, 171
Polytope, 160
Polytopic system, 159, 160, 167
Primary, 103, 107, 114, 127, 133
Primary actuator, ix, 39, 103, 104, 106, 110, 113–117, 120, 123

Primary control surface, ix, 52, 72, 115, 123, 126, 128, 131, 136, 140, 146
Projection based method, 9
Projection operator, 19, 30
Propulsion-control, 179
Pseudo-inverse, 11, 41, 43, 44, 66, 85, 108, 153
Pseudo-sliding, 25, 57, 72

R
Range space, xiii, 18, 27, 28
Reachability condition, 18, 20, 21, 23, 24, 31–33, 48, 69, 70, 92, 112, 113, 133
Reaching phase, 17, 27, 30, 32, 34, 35, 44, 66, 108
Reconfigurable control systems, 36
Reconfiguration mechanism, 3
RECOVER, 79, 124, 135, 170, 181
RECOVER model, xiv, 63, 71, 72, 78, 103, 113, 120, 123, 124, 133, 146, 160, 170, 171, 181, 183–185
RECOVER software, 73, 181
Reduced order system motion, 19
Redundancy, vii, x, 3, 6, 7, 11, 12, 39, 40, 51, 52, 59, 72, 81, 82, 104, 115, 146, 149, 166
Redundant actuators, 3, 7, 10, 12, 39, 49, 59, 60
Relay system, 17, 35
Reliability, vii, 1, 7, 11
Reliable control system, 7
Residual, 6
Retro-fit, 27, 32, 35, 103, 106, 120
Right pseudo-inverse, 10, 41, 43, 65, 87, 109, 151
Robust control, 7, 8, 10
Robustness, vii, 8, 17, 18, 25, 27, 34, 35, 81, 99, 131, 146, 156, 166
Rudder runaway, 181
Runaway (failure), 3, 99

S
Safety critical system, vii, 1, 6, 40
Schur complement, 51, 192, 193
Secondary, 103, 114, 127, 133
Secondary actuator, ix, 7, 103, 104, 107, 116, 117, 131
Secondary control surface, ix, 123, 126, 130, 146
Sensor fault, 1–3, 5, 12
Sensor faults/failures, 3
Sigmoidal approximation, 25, 33, 57, 72, 98, 116, 162
Signum function, 20
SIMONA research simulator, x, xiv, 169, 170, 178, 179
Slack variable, 51, 71, 90, 160
Sliding surface, viii, xiii, 8, 17–21, 23, 25, 27, 30–32, 36, 44, 57, 67, 72, 91, 101, 107, 111, 152
Small gain theorem, 46, 47, 68, 88, 110, 111, 155, 159, 189, 190
Smooth, 25, 36, 57, 72, 98, 116, 162, 163
Stabiliser runaway, 163, 166, 172, 175, 181
Stability analysis, viii, ix, 5, 43, 45, 46, 59, 63, 64, 68, 78, 81, 87, 100, 109, 110, 154, 155, 190
Stability condition, viii, ix, 47, 50, 59, 69, 70, 88, 95, 115–117, 159, 160, 162, 190
State feedback, ix, 27–29, 31, 43, 103, 105, 113–115, 120, 150, 159, 160, 167
Strict feedback form, 125, 130
Switching function, xiii, 17, 18, 23, 25, 29, 30, 33, 34, 44, 66, 83, 107, 120, 152, 153, 163, 166, 173, 175
Switching matrix, 19, 23, 29
Symmetric matrix, 44, 70
Symmetric positive definite, xiv, 33, 50, 89, 190
Symmetry, 30, 44, 84
Synthesis procedure, viii, 39

T
Threshold, 6, 56
Time-varying sliding surface, 131
Tracking performance, 59, 73, 98, 99, 136, 140, 143, 163, 166, 173, 175, 178
Transfer function, 46, 47, 68, 110, 190
Transport aircraft, 167
Trim point, 123, 183

U
Uncertainty, 18–20, 27, 29, 32, 40, 45, 66, 68, 86, 94, 136, 143, 153, 154
Unit vector, 20, 25, 48, 116, 158
Unknown input observer, ix, xiv, 6, 11, 81, 83, 84, 100, 101, 167
Unmatched uncertainty, viii, 28, 30–32, 44, 45, 63, 78, 109, 153

V
Variable structure control, xiv, 17, 35
Virtual control input, xiii, 41, 44, 65, 151
Virtual control law, ix, 11, 65, 78, 90, 149, 150, 152, 155
Virtual input matrix, 44

W
Washout filter, 113–115
Weighting matrix, 5, 63, 82, 104, 150
Wind, 63, 72, 78
Wind and gust, 72
Wind tunnel, 124